

The effect of chemical disorder on the gap of $\text{Hf}_x\text{Zr}_{1-x}\text{S}_3$ solid solutions

This article has been downloaded from IOPscience. Please scroll down to see the full text article.

1989 J. Phys.: Condens. Matter 1 1329

(<http://iopscience.iop.org/0953-8984/1/7/015>)

View [the table of contents for this issue](#), or go to the [journal homepage](#) for more

Download details:

IP Address: 171.66.16.90

The article was downloaded on 10/05/2010 at 17:48

Please note that [terms and conditions apply](#).

The effect of chemical disorder on the gap of $\text{Hf}_x\text{Zr}_{1-x}\text{S}_3$ solid solutions

R Gagnon, S Jandl and M Aubin

Centre de Recherche en Physique du Solide, Groupe de Recherches sur les Semiconducteurs et Diélectriques, Université de Sherbrooke, Sherbrooke, Québec J1K 2R1, Canada

Received 24 May 1988, in final form 19 August 1988

Abstract. Single crystals of a low-dimensional semiconducting system ($\text{Hf}_x\text{Zr}_{1-x}\text{S}_3$), whose lattice parameters do not vary significantly with composition, were prepared. It is expected that the band-gap variation will be dominated by chemical disorder and deviate from the usual parabolic behaviour. Our thermorefectance measurements at 70 K show in fact an unusual behaviour, the excitonic transitions being almost constant for $x = 0$ to $x \approx 0.6$ and varying linearly for $x > 0.6$. This deviation from the usual behaviour may possibly be explained by percolation phenomena.

1. Introduction

For many years, alloy semiconductors of the form $\text{A}_x\text{B}_{1-x}\text{C}$ have been assumed to satisfy the virtual crystal approximation (VCA) where the individual compounds AC and BC lose their chemical and structural identities and are replaced by a hypothetical crystal with an average lattice constant [1] which varies linearly with the concentration x (Végard's rule). This model therefore implies equal bond lengths between anions and cations. Turning to the electron energy bands of these alloys, the fundamental gap (and higher-energy transitions) display a deviation from linearity as one varies the composition. This deviation generally leads to a gap which is smaller than that resulting from a linear interpolation between the constituent compounds [2]. In general, one may fit the reduction in band gap to an empirical law of the form $bx(1-x)$, where b is called the bowing parameter and takes on values of about 0.9 eV for III–V alloys. The discovery of a bimodal distribution of nearest-neighbour bond lengths by EXAFS in $\text{In}_{1-x}\text{Ga}_x\text{As}$ alloys [3] has necessitated a re-evaluation of the VCA and of the physical origins of the bowing parameter. Although these results provided a new impetus in the study of semiconducting alloys, evidence of a bimodal behaviour of phonon energies in these materials had been seen previously by Raman and transport measurements [4, 5]. This evidence concerned phonon energies; nevertheless the information so obtained was not as direct as that found from EXAFS.

One of the studies following this discovery explained the results by the 'principle of conservation and transferability of chemical bonds' [6]. Most of the observed bowing in semiconducting alloys would thus be explained by the bond alternation. A molecular CPA calculation [7] showed that chemical disorder and bond length variations both

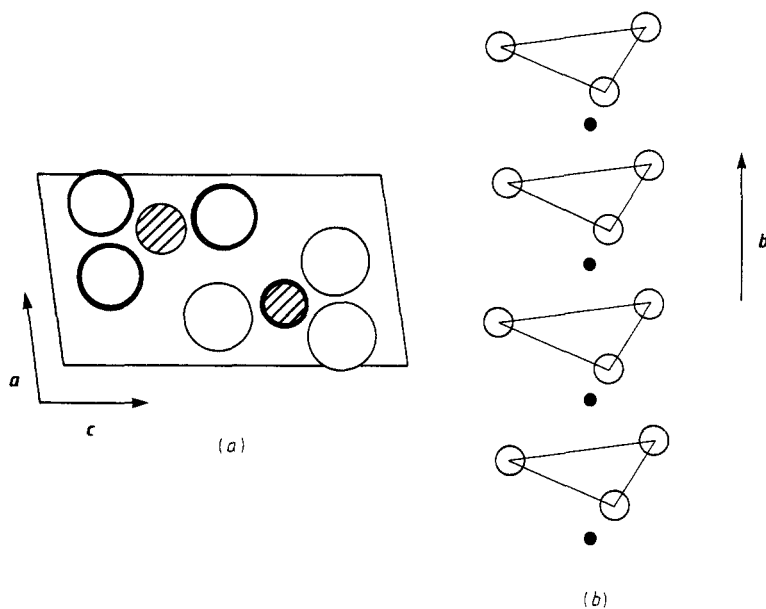


Figure 1. (a) The crystal structure of MS_3 ($M = \text{Hf, Zr}$) projected along the *b* axis. Metal atoms are indicated by hatched circles and sulphur by open circles. Atoms with heavy contours are at $y = \frac{1}{4}$ and those with light contours at $y = \frac{3}{4}$. (b) A chain of MS_3 along the *b* axis.

contribute significantly in $\text{In}_{1-x}\text{Ga}_x\text{As}$ alloys. It therefore seems useful to perform experiments which could isolate these two factors. The theoretical analysis could be simplified and the number of adjustable parameters reduced. For example, one could eliminate the bond length variations in an alloy system with almost constant lattice parameters, particularly if this system were of low dimensionality to reduce even further complicated interactions. These are stringent requirements but at least one case exists: $\text{Hf}_x\text{Zr}_{1-x}\text{S}_3$ solid solutions.

We have grown such crystals with various *x*-values and have measured the thermorefectance (TR) at 70 K. Only chemical disorder should determine the band-gap variation. The behaviour is unusual and may be understood by invoking percolation theory applied to band-structure calculations.

2. $\text{Hf}_x\text{Zr}_{1-x}\text{S}_3$ solid solutions

The crystallographic monoclinic structure of these compounds illustrated in figure 1 has been described in detail in [8] and [9]. Roughly speaking, they are made up of weakly coupled pairs of chains. There are eight atoms per unit cell. Each chain in a pair is weakly coupled through van der Waals forces to its companion.

A chain is made up of a perfectly ordered sublattice of M atoms (either Zr or Hf). In between every pair of M atoms, there are sulphur atoms on an isosceles triangle whose plane is perpendicular to the chain axis. The lattice parameters of ZrS_3 and HfS_3 are, respectively, $a = 5.124 \text{ \AA}$, $b = 3.624 \text{ \AA}$, $c = 8.980 \text{ \AA}$, $\beta = 97.28^\circ$ and $a = 5.092 \text{ \AA}$, $b = 3.595 \text{ \AA}$, $c = 8.967 \text{ \AA}$, $\beta = 97.38^\circ$. According to the x-ray results, the variation in the

average unit-cell dimensions with concentration x follows Végard's rule to a good approximation, even if the variations are extremely small [10].

In [11] the polarised optical absorption spectra of ZrS_3 and HfS_3 which showed a dichroism effect and apparent excitonic features are reported. In [12] resonance Raman spectra of HfS_3 and ZrS_3 powders [13] were obtained within the contour of the lowest allowed excitonic transition.

Band-structure calculations [14], optical absorption spectra [15] and TR [16] assign an indirect band gap for both ZrS_3 and ZrSe_3 . Experimental evidence for the HfS_3 band-gap origin is, however, still lacking.

The pseudo-binary alloys $\text{Hf}_x\text{Zr}_{1-x}\text{S}_3$ have been investigated by means of Raman scattering [10]. Phonon energy shifts with increase in x were found to be very small, reaching maximum values of about 10 cm^{-1} .

In this work, we report polarised TR spectra of HfS_3 and the mixed crystals $\text{Hf}_x\text{Zr}_{1-x}\text{S}_3$. The major features of this family are associated with direct and indirect excitonic transitions, which demonstrate an unusual energy variation with the compositional parameter x .

3. Experimental procedure

3.1. Crystals

The dimensions of the samples used in the present work were about $10 \text{ mm} \times 2 \text{ mm} \times 30 \mu\text{m}$, including the mixed crystals. Crystals were grown by iodine chemical transport reaction, taking advantage of the complete range of solid solubility. It is worth noting that the hafnium powder used to grow the crystals contained about 2–3% Zr, as specified by the supplier. Even though the lattice parameters a , b and c do not change significantly throughout the composition to allow us to determine x , x-ray spectra indicate that the solid solution is indeed formed. An important increase in the structure factor $S(003)$ with increasing x was observed. Figure 2 shows, as an example, three representative spectra obtained from monocrystals. The structure factor is expressed as

$$S(00l) = \sum_{j=1}^8 f_j \exp(-i2\pi lz_j) \quad (1)$$

where f_j is the atomic (ionic) form factor of the ions in the unit cell (six chalcogen and two metal ions) and z_j the position component of the j th ion in the direction perpendicular to the layers (parallel to the c axis). In the mixed compounds the form factor of the metal ions is

$$f(x) = xf(\text{Hf}^{4+}) + (1-x)f(\text{Zr}^{4+}). \quad (2)$$

We found that the structure factor $S(003)$ is very small in ZrS_3 compared with its value in HfS_3 , whereas this is not the case for $l = 1, 2$ or 4 . Also the peak for $l = 5$ is important in ZrS_3 and weak in HfS_3 . The behaviour for the theoretical peak amplitude ratio $|S(003)|^2/|S(002)|^2$ is somewhat linear and this is what is observed experimentally to within a few per cent. From these results, we conclude that the solid solution is in fact formed with the nominal values of x . This is of great importance when interpreting the variation with x of the electronic transition energies.

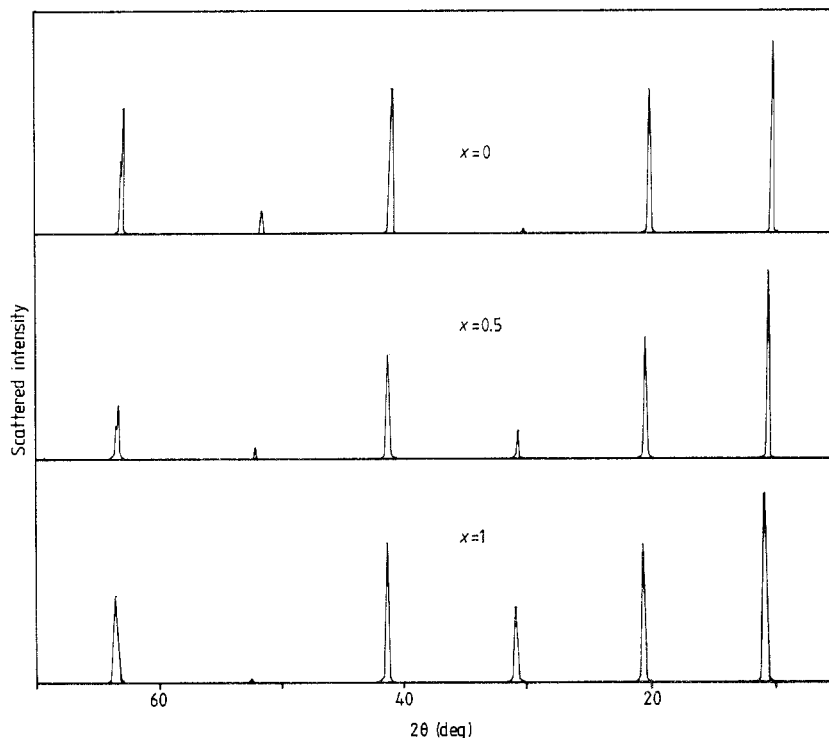


Figure 2. X-ray diffraction spectra of three monocrystals of $\text{Hf}_x\text{Zr}_{1-x}\text{S}_3$. $\theta = 0$ represents a parallel incidence of the x-ray beam with respect to the (a, b) plane.

3.2. Thermoreflectance

The temperature modulation ΔR of the reflectivity is observed with polarised light near normal incidence in the photon energy range 1.4–3.6 eV, at a temperature of around 70 K. A tungsten lamp is used as light source. Light is passed first in a Jarrell–Ash 0.5 m monochromator, with a 1180 grooves mm^{-1} grating, and then through a quartz polariser. The resolution at the monochromator output is estimated at 2 Å. Monochromatic light is incident on a sample mounted in an evacuated chamber, fixed on a cold finger at the bottom of a closed-cycle refrigerator. The reflected beam is then focused on a photomultiplier tube. The sample temperature is modulated at a frequency around 2 Hz by means of a commercial heater fixed between the sample and the cold head. Typically, the amplitude of the modulation is of the order of 2–3 K. Standard measurement techniques are carried out by using a lock-in amplifier to obtain the $\Delta R/R$ signal.

4. Results

4.1. TR spectra of the pure compounds

The TR spectra have been published recently for ZrS_3 with $E \parallel b$ and $E \perp b$ [16]. Here we focus our attention on the parallel polarisation spectra because of the much weaker signal obtained for HfS_3 with $E \perp b$. In fact, as the direct transitions are concerned, no

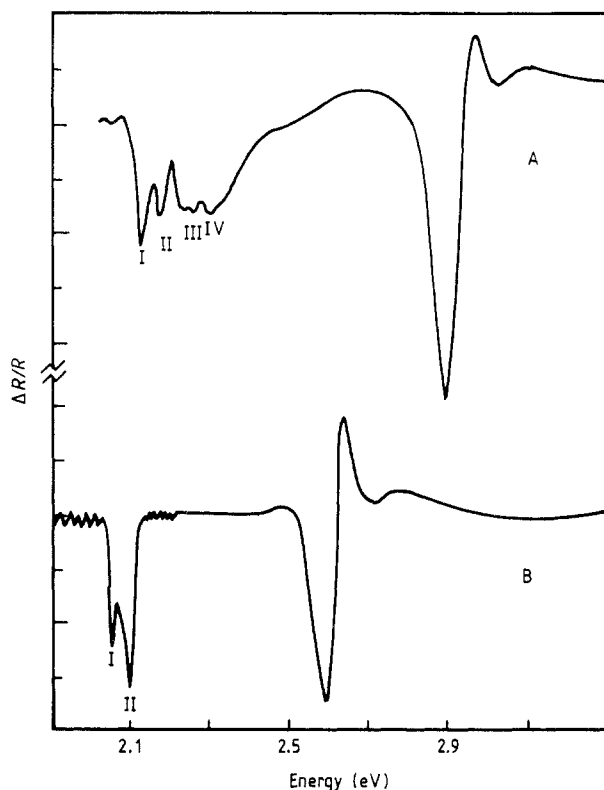


Figure 3. TR spectra obtained at 70 K for the polarisation $E \parallel b$: spectrum A, HfS_3 ; spectrum B, ZrS_3 .

excitonic peak was observed for both compounds with $E \perp b$. Figure 3 presents the TR spectra of ZrS_3 and HfS_3 . Indirect excitonic transitions are observed in the 2.0–2.4 eV region and a direct excitonic transition is responsible for the next important structure, at 2.59 eV in ZrS_3 and 2.91 eV in HfS_3 . In addition to the energy shift, the main difference between the two spectra is the presence of two additional much larger peaks in the indirect-gap region of HfS_3 .

As for ZrS_3 , the low-energy peaks in the HfS_3 spectrum are associated with indirect transitions. Peak I at 2.135 eV corresponds to an impurity-assisted transition and its position corresponds to the exciton energy, i.e. the wavevector conservation is realised without energy transfer to the crystal [17, 18]. Peak II at 2.179 eV refers to a phonon emission process, implying an energy difference between peaks I and II which represent a zone-edge phonon energy, 42 meV in ZrS_3 and 44 meV in HfS_3 .

The thickness dependence of peaks III and IV indicates their back-reflection origin too. Much larger than peaks I and II, they are associated with indirect transitions involving bands of other directions of the Brillouin zone.

The direct excitonic features are very similar in shape, width and amplitude for the two compounds. A direct comparison with the ZrS_3 structure [16] is sufficient to extract the exciton energy of HfS_3 , $E_{\text{ex}} = 2.84$ eV. The maximum of the absorption coefficient and the interface reflectivity variations are close enough for each to produce this similarity. In particular, it turns out from the curve-fitting procedure performed in [16] that a shift of 70 meV exists in ZrS_3 between the TR peak and the exciton transition

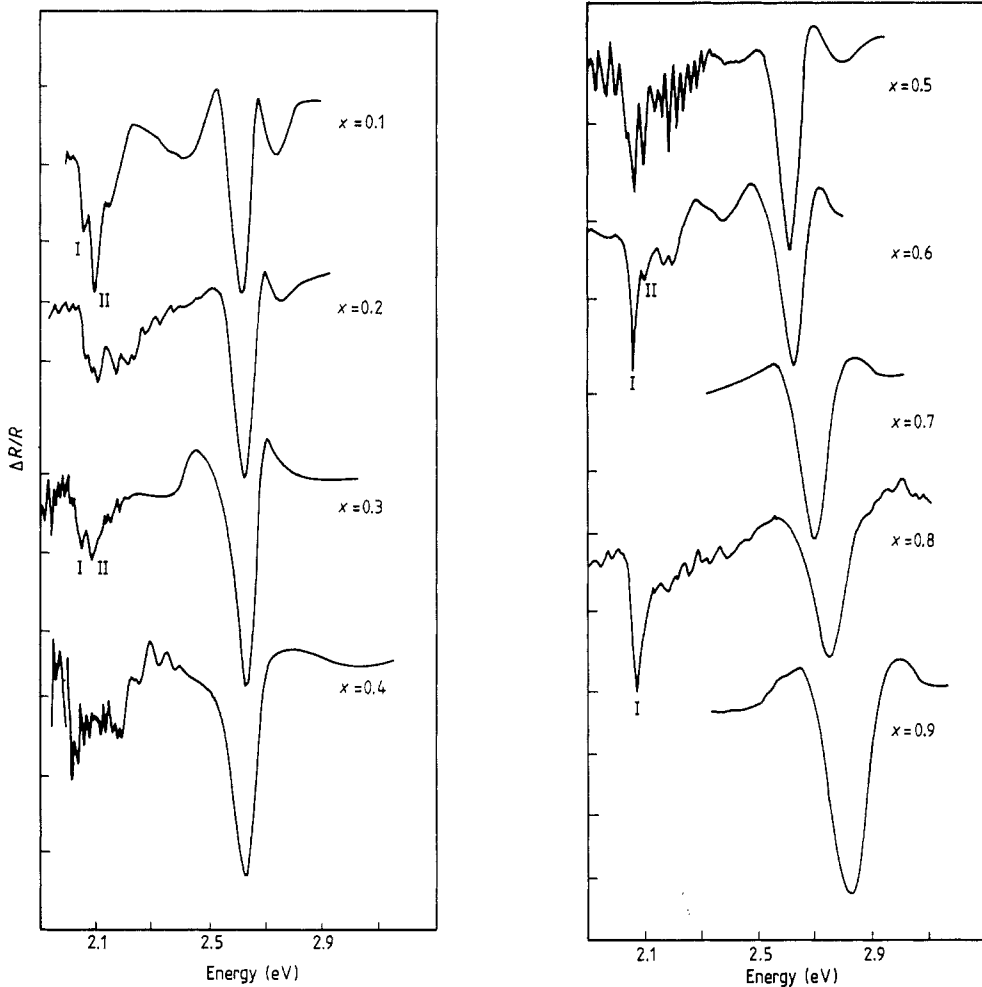


Figure 4. TR spectra, at 70 K, of the solid solution $\text{Hf}_1\text{Zr}_x\text{S}_3$, with $E \parallel b$.

energy. The same shift was obtained for HfS_3 in the present work. Thus, for the mixed compounds, it was assumed that again the same shift exists for lack of a better approximation.

4.2. Mixed compounds

The TR structures are easily recognisable in the mixed compounds. Figure 4 presents the TR spectra of nine binary compositions, with $E \parallel b$. For $E \perp b$, no excitonic structures were observed for the direct-transition region. The amplitude of the $\Delta R/R$ signal remains approximately constant for all the mixed compounds, i.e. about five times weaker than in the pure compounds, but always much beyond the detection limit. Also, the observation of peaks in the indirect-gap region of $\Delta R/R$ is very sensitive to the crystal thickness as well as to its uniformity. For these reasons, these peaks were not always present in the spectra, being sometimes partially or completely hidden by the inter-

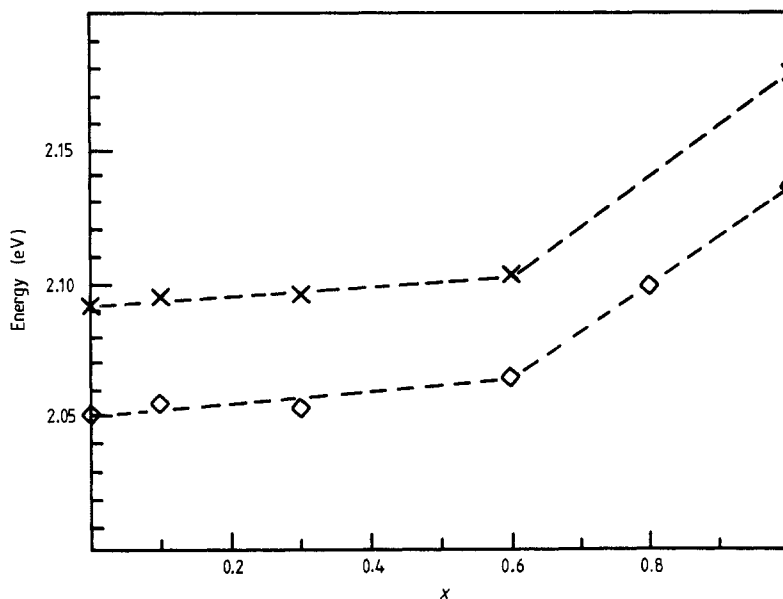


Figure 5. Variation with x of the indirect excitonic energies in $\text{Hf}_x\text{Zr}_{1-x}\text{S}_3$: \diamond , peak I, impurity-assisted transitions; \times , peak II, phonon-assisted transitions.

ference fringes. Nevertheless the data are sufficient to show a clear composition dependence of the indirect peaks energies, as shown in figure 5.

The only way to explain the presence of indirect peaks is to invoke exciton formation, because a square-root singularity is necessary to produce such a modulated back-reflection peak [19]. This is good evidence that excitons survive in our studied alloys.

As in the pure compounds, the low x -values ($0.1 < x < 0.6$) show the impurity-assisted (peak I) and the phonon-assisted (peak II) transitions. A gradual disappearance of peak II is observed, this peak being very small for $x = 0.6$ and undetected for $x = 0.8$.

In many III-V indirect-gap binary alloys [18], the impurity-assisted component of the absorption coefficient becomes greater as the 'doping' concentration increases. This phenomenon would explain the increase in peak I, the superimposed phonon emission component becoming much smaller and undetected for $x = 0.8$. Peak II reappears between $x = 0.9$ and $x = 1$. It is worth noting that the maximum width of the direct excitonic peak is reached for this particular composition, reflecting a maximum for the effective disorder. This value is far away from the expected value at $x = 0.5$, where the substitutional disorder is maximum.

The energy difference between peaks I and II is approximately constant in the mixed crystals: 42 ± 2 meV. This result is consistent with previous work on Raman scattering, because the nearest $k = 0$ phonon (at about 42 meV) displays a one-mode behaviour with a total shift of almost 1 meV [10].

The direct excitonic peak was present for all the compositions that we studied. Its energy position and width were reproducible for many samples of the same growth run. The results are shown in figure 6. Uncertainties in these peak energies are greater than in the indirect region because of their large width (about 0.1 eV) with respect to the total shift (about 0.3 eV). Nevertheless the error bars on the experimental points are of the order of the size of the symbols in this figure.

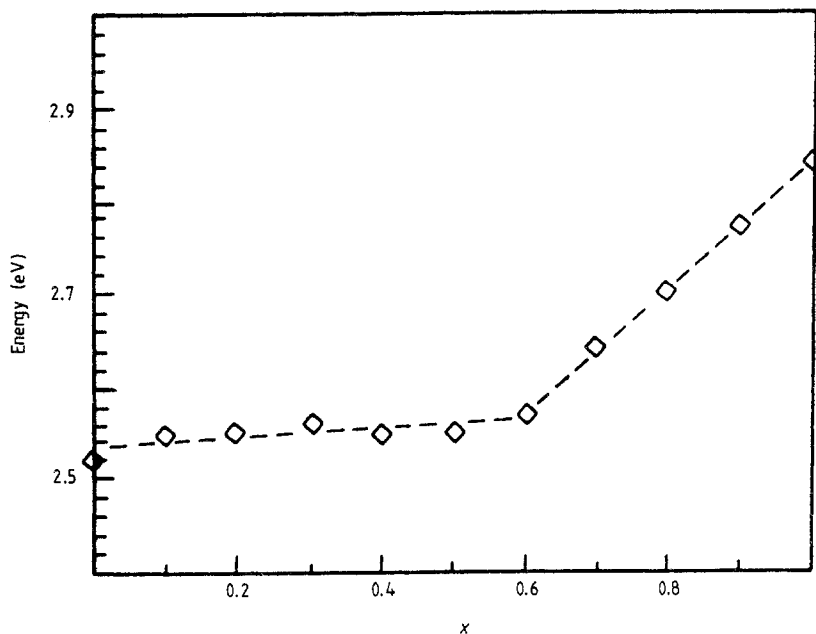


Figure 6. Transition energies of $\text{Hf}_x\text{Zr}_{1-x}\text{S}_3$ in the direct-gap region.

As observed in figures 5 and 6, both the direct and the indirect gaps define two straight lines. One varies quite slowly from $x = 0$ to $x = 0.55$ and the other has a much more rapid linear variation from $x > 0.55$ to $x = 1$. It was not possible to obtain a satisfactory fit of these data with a parabola. A similar but less pronounced example of this behaviour has been observed in the $L_{6c}-L_{4,5v}$ transition of $\text{Cd}_x\text{Hg}_{1-x}\text{Te}$ alloys [20, 21]. The transition energy begins with a linear variation before assuming the usual parabolic behaviour. $\text{Cd}_x\text{Hg}_{1-x}\text{Te}$ alloys also have a small variation in lattice parameter but are not low dimensional.

In our case, chemical disorder which produces two linear regimes for the gap is different from the bowing behaviour with quadratic dependence on x as usually suggested. According to [14] in which the electronic band structure of ZrSe_3 , which has a unit cell similar to those of ZrS_3 and HfS_3 , was calculated the trend of an increasing band gap between ZrS_3 and HfS_3 is understood as an increasing overlap between chalcogen p- and metal d-like wavefunctions.

The sudden increase in the gap as observed in the present experiment is reminiscent of 'percolation-type' phenomena. The percolation threshold for two-dimensional site percolation is 0.59, coincidentally close to the value of x where our change in slope occurs. The occupation of the MS_3 'sites' by $\text{M} \equiv \text{Zr}$ with probability $1 - x$ or by $\text{M} \equiv \text{Hf}$ with probability x would be a true percolation problem in the limit where one is studying classical objects having opposite properties (e.g. conducting as against insulating). In the actual quantum case under discussion, even if the properties of the two species are not very different, it is possible that a sudden change in the functional dependence of x occurs. For example, in the problem of Anderson localisation, it is known that the localisation transition occurs at a finite value of the difference in site energies in three dimensions.

5. Conclusion

We have found a low-dimensional alloy system in which the bond lengths do not vary significantly with composition. The energy gaps as measured through the indirect and direct excitons do not vary in the usual parabolic manner. Presumably chemical disorder would be the only important factor determining this behaviour. Our experimental results thus constitute an interesting basis for a detailed theoretical analysis which considers both band-structure calculations and percolation phenomena.

Acknowledgments

The authors gratefully acknowledge useful discussions with A-M Tremblay. This work was partly financed by the Research and Development Branch of the Department of National Defence under Contract 8SD85-00313. One of us (RG) would like to thank the Natural Sciences and Engineering Research Council for financial support.

References

- [1] Parmenter R H 1955 *Phys. Rev.* **97** 587
- [2] Cardona M 1963 *Phys. Rev.* **129** 69
- [3] Mikkelsen J C and Boyce J B 1983 *Phys. Rev. Lett.* **49** 1412
- [4] Jandl S, Harbec J Y and Carlone C 1978 *Solid State Commun.* **27** 1441
- [5] Perluzzo G, Jandl S, Aubin M and Girard P E 1978 *Solid State Commun.* **27** 1437
- [6] Zunger A and Jaffe J E 1983 *Phys. Rev. Lett.* **51** 662
- [7] Hass K C, Lempert R J and Ehrenreich H 1984 *Phys. Rev. Lett.* **52** 77
- [8] Krönert W and Plieth K 1965 *Z. Anorg. Allg. Chem.* **336** 207
- [9] Brattås L and Kjekshus A 1972 *Acta Chem. Scand.* **26** 3441
- [10] Nouvel G, Zwick A, Rennucci M A and Kjekshus A 1985 *Phys. Rev. B* **32** 1165
- [11] Schairer W and Shafer M W 1973 *Phys. Status Solidi a* **17** 181
- [12] Gwet S P, Mathey Y and Sourisseau C 1984 *Phys. Status Solidi b* **123** 503
- [13] Sourisseau C and Mathey Y 1980 *Chem. Phys. Lett.* **74** 128
- [14] Myron H W, Harmon B N and Khumalo F S 1981 *J. Phys. Chem. Solids* **42** 263
- [15] Kurita S, Staehli J L, Guzzi M and Lévy F 1981 *Physica B* **105** 169
- [16] Provencher R, Gagnon R, Jandl S and Aubin M 1988 *J. Phys. C: Solid State Phys.* **21** 615
- [17] Kanzaki H and Sakuragi S 1970 *J. Phys. Soc. Japan* **29** 924
- [18] Strehlow R 1978 *Phys. Status Solidi b* **86** 311
- [19] Gagnon R, Bernier G, Jandl S and Aubin M 1987 *Solid State Commun.* **64** 361
- [20] Hass K C, Ehrenreich H and Velicky B 1983 *Phys. Rev. B* **27** 1088
- [21] Viña L, Umbach C, Cardona M and Vodopyanov L 1984 *Phys. Rev. B* **29** 6752